

Proceeding Paper

Conductivity Transport Mechanisms of Solution-Processed Spinel Nickel Cobaltite-Based Hole Transporting Layers and Its Implementation as Charge Selective Contact in Organic Photovoltaics [†]

Apostolos Ioakeimidis ¹, Aristeidis Kottaras ², Dimitrios Karageorgopoulos ², Efstathia Christia ³, Sotirios Sakkopoulos ², Evangelos Vitoratos ², Stelios A. Choulis ¹ and Ioannis T. Papadas ^{3,*}

¹ Molecular Electronics and Photonics Research Unit, Department of Mechanical Engineering and Materials Science and Engineering, Cyprus University of Technology, 45 Kitiou Kyprianou Str., Limassol 3041, Cyprus; a.ioakeimidis@cut.ac.cy (A.I.); stelios.choulis@cut.ac.cy (S.A.C.)

² Department of Physics, University of Patras, 26504 Patras, Greece; ariskottaras@gmail.com (A.K.); dimitriskarageorgopoulos@gmail.com (D.K.); ssakkopoulos450@gmail.com (S.S.); vitoratos@upatras.gr (E.V.)

³ Department of Public and Community Health, School of Public Health, University of West Attica, 11521 Athens, Greece; echristia@gmail.com

* Correspondence: ipapadas@uniwa.gr

[†] Presented at the 16th International Conference on Meteorology, Climatology and Atmospheric Physics—COMECAP 2023, Athens, Greece, 25–29 September 2023.

Abstract: The electrical properties of solution-processed spinel nickel cobaltite (NiCo₂O₄) nanoparticulated-based metal oxide hole transporting layers are investigated using conductivity and Hall effect measurements. The mechanism of electrical conductivity of NiCo₂O₄-based electronic films as a function of temperature indicates hopping-type carrier transport. We show that NiCo₂O₄ hole transporting layers (HTLs) have suitable conductivity, low toxicity, and relatively low processing temperature, parameters that are important for electronic materials specifications of high performance and environmentally friendly emerging photovoltaics. As a proof of concept, NiCo₂O₄ and Cu-SCN surface-modified NiCo₂O₄ are incorporated as HTLs for non-fullerene acceptor Organic Photovoltaics (OPVs), and the photovoltaic performance results of the corresponding OPVs are presented.

Keywords: metal oxides; NiCo₂O₄; combustion synthesis; conductivity; transport mechanisms; hall effect measurements; electrodes; organic photovoltaics



Citation: Ioakeimidis, A.; Kottaras, A.; Karageorgopoulos, D.; Christia, E.; Sakkopoulos, S.; Vitoratos, E.; Choulis, S.A.; Papadas, I.T.

Conductivity Transport Mechanisms of Solution-Processed Spinel Nickel Cobaltite-Based Hole Transporting Layers and Its Implementation as Charge Selective Contact in Organic Photovoltaics. *Environ. Sci. Proc.*

2023, 26, 63. <https://doi.org/10.3390/environsciproc2023026063>

Academic Editors: Konstantinos Moustiris and Panagiotis Nastos

Published: 25 August 2023



Copyright: © 2023 by the authors. Licensee MDPI, Basel, Switzerland. This article is an open access article distributed under the terms and conditions of the Creative Commons Attribution (CC BY) license (<https://creativecommons.org/licenses/by/4.0/>).

1. Introduction

To make the transition to low-carbon energy systems, research on solar energy technology that attempts to transform sunlight directly into electrical energy is essential [1]. Investigations to improve the efficiency and stability of emerging photovoltaic technologies have been accelerated by the rapid advances of innovative electronic materials in the field of material science.

Organic photovoltaics (OPVs) are one of the most promising emerging solar cell technologies due to their benefits regarding low solution processing manufacturing for large-scale roll-to-roll production and less impact on the environment after disposal in comparison to other photovoltaics technologies [2–8]. Recently, non-fullerene acceptors (NFAs) within the active layers of solution-processed organic photovoltaics (OPVs) have greatly improved their power conversion efficiency (PCE) in the range of 19% [9,10].

Hole-transporting layers (HTLs) and electron transport layers (ETLs) are essential interlayers in OPVs since they increase the collecting capabilities of hole and electron charges toward the anode and cathode electrodes, respectively, and, therefore, increase the power conversion efficiency (PCE) of OPVs [11,12]. However, the development of

appropriate charge-selective contacts between the active layer and the electrodes in OPVs presents challenges [13,14].

For the normal OPV device architecture, the most used conducting polymer HTL is the Poly(3,4-ethylenedioxythiophene)-poly(styrene sulfonate) (PEDOT:PSS) due to its low cost, limited toxicity, easy solution processing, and high work function (WF). However, due to its hygroscopic and acidic properties, PEDOT:PSS creates stability issues during solar cell operation under environmental conditions, which leads to the usage of p-type metal oxides as HTLs in OPVs instead, which in some cases provide improved lifetime performance due to their chemical and moisture resistance [7,15].

The most common p-type metal oxides that have been employed as HTLs in OPVs are MoO_3 , NiO, WO_3 , Fe_3O_4 , and CuO_x [16–20]. Nevertheless, despite their aforementioned advantages, they suffer from low electrical conductivity, which can limit the performance of the respective solar cell devices. Furthermore, high vacuum techniques for deposition, as well as temperatures above 400 °C in order to achieve enhanced metal oxide crystallinity, are usually required for their synthesis, resulting in increased device manufacturing costs and simultaneously restricting their application to flexible photovoltaic applications [21,22].

Nickel cobaltite (NiCo_2O_4) is an environmentally friendly p-type transparent conductive oxide (TCO) material with the following characteristics: a wide optical band gap (~2.4 eV), a deep-lying valence band (~5.3 eV) and a conductivity of two orders of magnitude greater than NiO and Co_3O_4 . Due to those reasons, nickel cobaltite is considered a reliable metal-oxide electronic material for use in optoelectronics [23].

We have previously reported the solution combustion-synthesized (SCS) of a smooth, compact, and functional electronic film of the highly conductive spinel nickel cobaltite (NiCo_2O_4) nanoparticles utilizing tartaric acid as a fuel to produce monodispersed particles with mean size of ~4 nm, which was successfully introduced as hole transporting layers in inverted perovskite solar cells (PVSCs) [24].

In this paper, we examine the implementation of neat and Cu-SCN surface-modified nickel cobaltite (NiCo_2O_4) as a hole transporting layer (HTL) on the performance of non-fullerene acceptor (PBDB-TF-T1 (T1): ITIC-4F) based OPVs that have been processed using the low-toxicity solvent O-xylene. Furthermore, we study the electrical characteristics of NiCo_2O_4 HTLs using D.C. conductivity measurements in the temperature range of 100 to 340 K. The above measurements allow us to identify “hopping-like” charge transport as the conductivity mechanism and calculate the “hopping” distance of the solution-processed nanoparticulate-based NiCo_2O_4 HTLs. Moreover, Hall voltage measurements were conducted, revealing the high charge carrier concentration of the NiCo_2O_4 . The thermal treatment of the NiCo_2O_4 HTLs of different thicknesses (80 nm and 120 nm) was evaluated at 340 K for 1.5, 3, 6, and 12 h thermal aging time. Finally, the initial performance of PBDB-TF-T1 (T1): ITIC-4F-based OPVs incorporating NiCo_2O_4 as hole transporting layers is demonstrated.

2. Materials and Methods

Materials: Pre-patterned glass-ITO substrates (sheet resistance 4 Ω /sq) were purchased from Psiotec Ltd. The PBDB-TF-T1 (T1) and ITIC-4F were purchased from Ossila Ltd., (Sheffield, UK) and all the other chemicals used in this study were purchased from Sigma Aldrich.

Synthesis of NiCo_2O_4 NPs films: To synthesize nickel cobaltite nanoparticles using the solution combustion method, 15 mL of 2-methoxy ethanol was mixed with 0.5 mmol of nickel(II) nitrate hexahydrate, 1 mmol of cobalt(II) nitrate hexahydrate, 1.5 mmol tartaric acid and 150 μL 69% wt nitric acid, and stirred up for 30 min at 60 °C. The ITO substrates were sonicated for 10 min in acetone and isopropanol, dried with N_2 blow, and before use, they were UVO_3 treated for 20 min. NiCo_2O_4 precursor films were formed on ITO substrate using a doctor blade and then left to dry on a hot plate for 30 min at 100 °C. The spinel oxide (NiCo_2O_4) nanoparticulate films were combustion synthesized by heating

the precursor films in a preheated oven at 250 °C in ambient air for 4 h [24]. For the Hall measurement the films were fabricated on glass instead of ITO.

Device fabrication: The normal organic solar cells under study were ITO/NiCo₂O₄-NPs/(w/ or w/o Cu-SCN)/T1:ITIC-4F/Ca/Al. The ITO/NiCo₂O₄ hole transporting layers (HTL) were prepared as described above. Cu-SCN was spin-coated on NiCo₂O₄ from a 10 mg/mL diethyl-sulfide solution at 3000 RPM without any further treatment. The active layer T1:ITIC-4F (1:1.2% wt) was blade coated from a 20 mg/mL solution in O-xylene, resulting in a film thickness of ~110 nm and annealed for 10 min at 100 °C in the glovebox. Finally, 10 nm Ca and 100 nm Al layers were thermally evaporated using a shadow mask to finalize the devices, giving an active area of 0.9 mm². Encapsulation was applied directly after evaporation in the glove box using a glass coverslip and an Ossila E131 encapsulation epoxy resin activated using 365 nm UV irradiation.

Characterization: The current density-voltage (J-V) characteristics were obtained with a Botest LIV Functionality Test System. Forward scans were measured with 10 mV voltage steps and 40 msec of delay time. For illumination, a calibrated Newport Solar simulator equipped with an Xe lamp was used, providing an AM1.5G spectrum at 100 mW/cm² as measured using a certified Oriel 91150V calibration cell. A shadow mask was attached to each device prior to measurements to accurately define the corresponding device area. The four-probe method was used to measure the D.C. conductivity versus temperature in a cryostat containing inert He gas from 100 to 340 K. Platinum pressure contacts were used. The current to the sample was supplied by a Hewlett Packard 6177C constant current source, and the voltages and current were measured using a Keithley 195A digital multimeter and a Thurby 1905a intelligent digital multimeter. The temperature was stabilized to ±2 K via an Oxford ITC4 intelligent temperature controller. Nickel cobaltite films of 80 nm and 120 nm thickness, respectively, were thermally treated at 70 °C in a thermostated oven under ambient air for different aging times (t = 1.5, 3, 6, and 12 h). After each heat treatment, the conductivity versus temperature was determined. These successive measurements yield a set of $r = r(T)$ curves, and the entire process is repeated until conductivity reaches saturation. The Hall measurements were performed at room temperature using the Van der Pauw configuration and a magnetic field of 1T (ezHEMS, NanoMagnetics).

3. Results and Discussion

3.1. D.C. Conductivity and Hall Effect Measurements of NiCo₂O₄ Electronic Films

We investigated the electrical properties of the material using D.C. conductivity studies. The D.C. conductivity of NiCo₂O₄ films of 80 nm (Figure 1a) and 120 nm (Figure 1b) thickness was examined in the temperature range of 100 to 340 K. The thermal treatment of the samples took place at 340 K for 1.5, 3, 6, and 12 h. By increasing the time of thermal aging, a shift of the curve to lower conductivity values appears, which indicates that this “soft thermal treatment” has a measurable impact on the conductivity and is thus attributed to internal structural change.

The conductivity was thermally activated, and its dependence versus temperature is studied in the frame of Variable Range Hopping (VRH) and Nearest Neighbour Hopping (NNH). In Mott’s model, the hopping distance is given by $R = \left[\frac{9}{8\pi\alpha T k_B N(E_F)} \right]^{\frac{1}{4}}$, where the localization length $\alpha = \frac{1}{r_0}$ and $r_0 \sim \frac{R}{2} \rightarrow \alpha \approx \frac{1}{8.14} \approx 0.125 \text{ \AA}^{-1} \approx 0.125 * 10^8 \text{ cm}^{-1}$ [25]. From the equation: $T_0 = \left[\frac{18}{r_0^3 k_B N(E_F)} \right]$, we can calculate the density of states $N(E_F)$, $N(E_F) = \left[\frac{18}{r_0^3 k_B T_0} \right] \sim 5.1 * 10^{-5} \frac{\text{electronic states}}{\text{\AA}^3 \text{ ev}}$, where $T_0 \sim 80 * 10^5$ K. In such a case, taking $T = 300$ K, we find for the hopping distance: $R \sim 39 \text{ \AA}$. This value is about four times the lattice parameter, in good accordance to Dillep K. et al. [26].

The solution combustion synthesis of NiCo₂O₄ implies the formation of nanoparticles (NPs). The typical grain dimensions range from 3.5 to 5 nm without avoiding the presence of amorphous microregions [24]. The conductivity versus temperature measurements, in the range of 100–340 K, reveal a Mott’s conduction according to the formula: $\sigma = \sigma_0 \exp$

$[-(T_0/T)^{0.25}]$. The same model also holds after heat treatment of the samples for $t = 1.5, 3, 6,$ and 12 h. For the thinner nickel cobaltite film of 80 nm, a short heating of 1.5 h improves the conductivity, though longer heat treatment gradually displaces the conductivity curve to lower values (Figure 1a). For the thicker nickel cobaltite film of 120 nm, a monotonic decrease in the conductivity values occurs, indicating that the thickness exerts influence on the way that the thermal heating affects the internal structure of the material (Figure 1b).

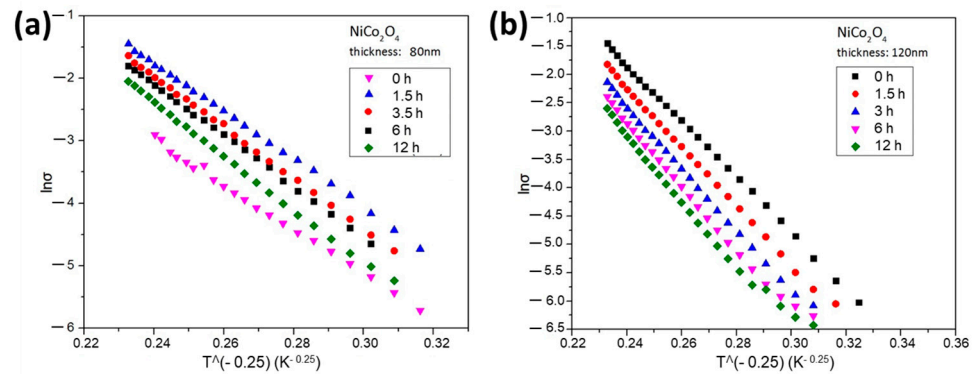


Figure 1. The $\ln \sigma = f(T^{-0.25})$ measurements for (a) 80 nm thickness of NiCo_2O_4 film and (b) 120 nm thickness of NiCo_2O_4 film, heated at 70 °C under ambient air conditions for aging times $0, 1.5, 3, 6$ and 12 h, respectively.

In polycrystalline metal oxide films, the grain boundaries can act as deep traps and cause the film’s conductivity to decay or recover slowly. However, regarding NiCo_2O_4 films, Hu et al. 2011 have proposed that the aforementioned deep trap defect on the photo-response behavior has been avoided due to their short decay and recovery times, which may be attributed to their exceptional crystallinity, purity, and morphology of nanoparticles [27]. Due to the existence of physical boundaries between the NiCo_2O_4 nanoparticles, the charge transfer among them is “hopping-like” [28].

In general, a “hopping-like” transport is stated by the temperature dependency of the experimental measurements of the conductivity, where the parameter σ_0 is a measure of the conductivity, which is related to the interior of the grains of the material. The parameter T_0 , on the contrary, is a measure of the potential barrier height, as thermally activated carriers hop between localized states with distinct energies [29,30].

As seen in Figure 2, the values of σ_0 and T_0 increase after heat treatment at 70 °C during the first three hours for both nickel cobaltite films of 80 nm and 120 nm thickness, respectively. Specifically, regarding the thicker 120 nm NiCo_2O_4 film, it is depicted that the values of σ_0 range from $21 \times 10^3 \text{ S cm}^{-1}$ for $t = 0$ h to $30 \times 10^3 \text{ S cm}^{-1}$ for $t = 3$ h, while the values of T_0 increase from $59 \times 10^5 \text{ K}$ to $83 \times 10^5 \text{ K}$, respectively. Similar behavior is observed for the thinner 80 nm NiCo_2O_4 film during the first three hours whilst depicting 12 times lower values of σ_0 and about three times lower values of T_0 for $t = 3$ h in comparison to the thicker 120 nm NiCo_2O_4 film (Figure 2a,b). This indicates that there is an improvement in conduction mechanisms during the first three hours following a stabilization of the process, remaining nearly constant during the thermal treatment exceeding four hours, suggesting that the conductivity, in that case, is not affected by thermal aging. The charge carrier mobility and concentration of the solution combustion synthesized NiCo_2O_4 were obtained using a 1T magnet. The p-type NiCo_2O_4 films exhibit a high carrier concentration of $\sim 3.9 \times 10^{20} \text{ cm}^{-3}$ and a mobility of $\sim 7.4 \times 10^{-2} \text{ cm}^2/\text{V.s}$.

3.2. Normal Device Architecture OPVs with Neat NiCo_2O_4 and Cu-SCN Surface Modified NiCo_2O_4 HTLs

The above observation of suitable conductivity, low toxicity, and relatively low processing temperature of NiCo_2O_4 are important parameters for high-performance and environmentally friendly OPVs. In this section, we fabricate a normal device structure OPVs based on the T1:ITIC-4F active layer using NiCo_2O_4 and Cu-SCN surface-modified

NiCo₂O₄ HTLs. Importantly, for the processing of the presented OPVs, the low-toxicity solvent O-xylene is used instead of commonly used, replacing the high-toxicity halogenated solvents (e.g., chloroform, chlorobenzene) commonly used for reporting high-performance OPVs in the literature. Furthermore, both NiCo₂O₄ and Cu-SCN surface-modified NiCo₂O₄ HTLs, as well as the OPV active layer, were deposited using blade coating, which is a scalable technique compatible with the fabrication of large-area OPVs.

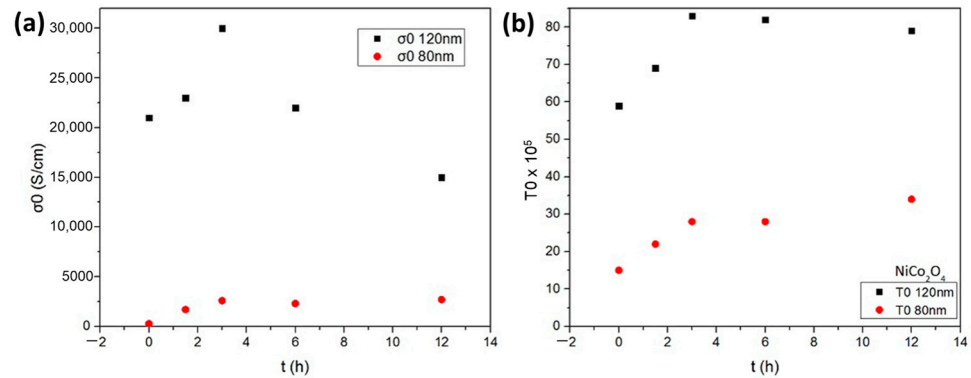


Figure 2. The parameters (a) σ_0 and (b) T_0 versus the aging time for 80 nm thickness of NiCo₂O₄ film and 120 nm thickness of NiCo₂O₄ film, respectively, during thermal treatment at 70 °C under ambient air.

Thus, the neat and Cu-SCN surface-modified NiCo₂O₄ HTLs were used as hole-transporting layers in OPVs with the following structure: ITO/HTL/T1:ITIC-4F/Ca/Al. Figure 3 presents the light J-V curves of the corresponding solar cells under 1 sun-simulated light (A.M.1.5) using neat NiCo₂O₄ and surface modified with Cu-SCN as HTLs. The respective photovoltaic parameters, open circuit voltage (Voc), short circuit current (Jsc), fill factor (FF), and power conversion efficiency (PCE) are presented in Table 1. The OPVs with neat NiCo₂O₄ HTL provide a PCE = 4.38%, with a Voc = 0.89 V, Jsc = 12.00 mA/cm² and FF = 40.75%. The proposed Cu-SCN surface treatment of the NiCo₂O₄ improves the PV parameters: a Voc = 0.92 V, Jsc = 15.06 mA/cm², and FF = 44.76% and thus improves the corresponding PCE value to 6.20%. The PCE enhancement is ascribed to the Cu-SCN surface treatment of the NiCo₂O₄ HTL that provides passivation of the surface defects of NiCo₂O₄, reducing the interface charge carrier recombination as it can be derived from the increased Voc value of the corresponding OPVs. Moreover, the Cu-SCN surface treatment of the NiCo₂O₄ HTL improves the electron-blocking properties of the bottom OPV electrode, resulting in increased Jsc and FF values for the corresponding OPVs. The above initial device performance results demonstrate the potential of NiCo₂O₄ and Cu-SCN surface-treated NiCo₂O₄ HTLs for the fabrication of environmentally friendly OPVs.

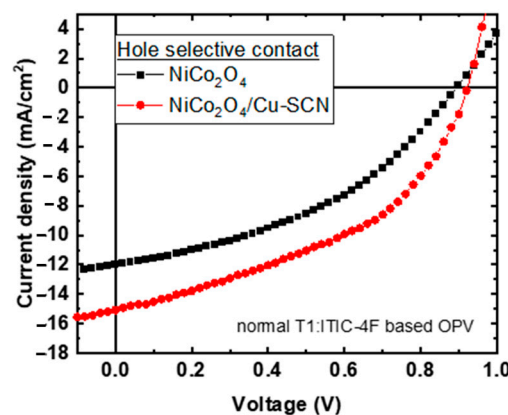


Figure 3. Light J-V curves of T1:ITIC-4F based OPVs with NiCo₂O₄ (black square) and NiCo₂O₄/Cu-SCN (red cycles) as hole transporting layers.

Table 1. PV parameters of the normal device architecture T1:ITIC-4F based OPV using NiCo₂O₄ and NiCo₂O₄/Cu-SCN as hole transporting layers.

HTL	Voc (V)	Jsc (mA/cm ²)	FF (%)	PCE (%)
NiCo ₂ O ₄	0.89	−12.00	40.75	4.38
NiCo ₂ O ₄ /Cu-SCN	0.92	−15.06	44.76	6.20

4. Conclusions

In conclusion, we studied the electrical properties of NiCo₂O₄ films using D.C. conductivity and Hall effect measurements. The D.C. conductivity measurements via a soft thermal aging treatment of NiCo₂O₄ films of different thicknesses (80 and 120 nm) that have been processed to identical conditions to NiCo₂O₄ HTLs incorporated within OPVs showed a detectable impact on the conductivity, which was accredited to internal structural change. Specifically, for the thinner nickel cobaltite HTL of 80 nm, a short heating time of 1.5 h increased the conductivity, whereas a prolonged heating time gradually shifted the conductivity curve to lower values, whilst for the thicker nickel NiCo₂O₄ HTL of 120 nm, the conductivity values decreased monotonically. Those measurements enabled us to identify a “hopping-like” charge transport as the primary mechanism that determines the conductivity and consequently calculate the “hopping” distance of solution-processed nanoparticulate-based NiCo₂O₄ HTLs. Moreover, hall effect measurements revealed a high carrier concentration of $\sim 3.9 \times 10^{20} \text{ cm}^{-3}$ and mobility of $\sim 7.4 \times 10^{-2} \text{ cm}^2/\text{V.s}$ for p-type NiCo₂O₄ HTLs. Furthermore, we examined the implementation of low toxicity NiCo₂O₄ and Cu-SCN surface modified NiCo₂O₄ as hole transporting layers on the performance of non-fullerene acceptor (T1:ITIC-4F) based OPVs that have been processed by blade coating using non-chlorinated solvents such as O-xylene and alcohols, thus giving the opportunity for the development of eco-friendly solution-processed OPVs. The initial reported solar cell device results for the proposed Cu-SCN surface treatment of NiCo₂O₄ HTL showed improved photovoltaics characteristics, yielding Voc = 0.92 V, Jsc = 15.06 mA/cm², and FF = 44.76%, and thus enhancing the corresponding PCE value to 6.20% compared to untreated NiCo₂O₄ HTL based OPVs with PCE of 4.38%.

Author Contributions: Conceptualization, S.A.C. and I.T.P.; methodology, A.I., A.K., D.K., E.C., S.S., E.V., S.A.C. and I.T.P.; formal analysis, A.I., A.K., D.K., E.C., S.S., E.V., S.A.C. and I.T.P.; investigation, A.I., A.K., D.K., E.C., S.S., E.V., S.A.C. and I.T.P.; data curation, A.I.; writing—original draft preparation, A.I., S.A.C. and I.T.P.; writing—review and editing, S.A.C. and I.T.P.; supervision, S.S., E.V., S.A.C. and I.T.P.; funding acquisition, S.A.C. All authors have read and agreed to the published version of the manuscript.

Funding: This research received no external funding.

Institutional Review Board Statement: Not applicable.

Informed Consent Statement: Not applicable.

Data Availability Statement: The data that support the findings of this study are available from the corresponding author upon reasonable request.

Conflicts of Interest: The authors declare no conflict of interest.

References

1. Kannan, N.; Vakeesan, D. Solar energy for future world: A review. *Renew. Sustain. Energy Rev.* **2016**, *62*, 1092–1105. [[CrossRef](#)]
2. ur Rehman, S.; Noman, M.; Khan, A.D.; Saboor, A.; Ahmad, M.S.; Khan, H.U. Synthesis of polyvinyl acetate/graphene nanocomposite and its application as an electrolyte in dye sensitized solar cells. *Optik* **2020**, *202*, 163591. [[CrossRef](#)]
3. Lin, Y.; Shao, Y.; Dai, J.; Li, T.; Liu, Y.; Dai, X.; Xiao, X.; Deng, Y.; Gruverman, A.; Zeng, X.C.; et al. Metallic surface doping of metal halide perovskites. *Nat. Commun.* **2021**, *12*, 7. [[CrossRef](#)] [[PubMed](#)]
4. Chen, Q.; Chen, L.; Ye, F.; Zhao, T.; Tang, F.; Rajagopal, A.; Jiang, Z.; Jiang, S.; Jen, A.K.Y.; Xie, Y.; et al. Ag-Incorporated Organic-Inorganic Perovskite Films and Planar Heterojunction Solar Cells. *Nano Lett.* **2017**, *17*, 3231–3237. [[CrossRef](#)]

5. Georgiou, E.; Ioakeimidis, A.; Antoniou, I.; Papadas, I.T.; Hauser, A.; Rossier, M.; Linardi, F.; Choulis, S.A. Non-Embedded Silver Nanowires/Antimony-Doped Tin Oxide/Polyethylenimine Transparent Electrode for Non-Fullerene Acceptor ITO-Free Inverted Organic Photovoltaics. *ACS Appl. Electron. Mater.* **2023**, *5*, 181–188. [[CrossRef](#)]
6. Hermerschmidt, F.; Choulis, S.A.; List-Kratochvil, E.J.W. Implementing Inkjet-Printed Transparent Conductive Electrodes in Solution-Processed Organic Electronics. *Adv. Mater. Technol.* **2019**, *4*, 1800474. [[CrossRef](#)]
7. Park, S.; Kim, T.; Yoon, S.; Koh, C.W.; Woo, H.Y.; Son, H.J. Progress in Materials, Solution Processes, and Long-Term Stability for Large-Area Organic Photovoltaics. *Adv. Mater.* **2020**, *32*, 2002217. [[CrossRef](#)]
8. Liu, S.; Yuan, J.; Deng, W.; Luo, M.; Xie, Y.; Liang, Q.; Zou, Y.; He, Z.; Wu, H.; Cao, Y. High-efficiency organic solar cells with low non-radiative recombination loss and low energetic disorder. *Nat. Photonics* **2020**, *14*, 300–305. [[CrossRef](#)]
9. Zhu, L.; Zhang, M.; Xu, J.; Li, C.; Yan, J.; Zhou, G.; Zhong, W.; Hao, T.; Song, J.; Xue, X.; et al. Single-junction organic solar cells with over 19% efficiency enabled by a refined double-fibril network morphology. *Nat. Mater.* **2022**, *21*, 656–663. [[CrossRef](#)]
10. Bao, S.; Yang, H.; Fan, H.; Zhang, J.; Wei, Z.; Cui, C.; Li, Y. Volatilizable Solid Additive-Assisted Treatment Enables Organic Solar Cells with Efficiency over 18.8% and Fill Factor Exceeding 80%. *Adv. Mater.* **2021**, *33*, 2105301. [[CrossRef](#)]
11. Po, R.; Carbonera, C.; Bernardi, A.; Camaioni, N. The role of buffer layers in polymer solar cells. *Energy Environ. Sci.* **2011**, *4*, 285–310. [[CrossRef](#)]
12. Li, Y.; Huang, X.; Ding, K.; Sheriff, H.K.M.; Ye, L.; Liu, H.; Li, C.-Z.; Ade, H.; Forrest, S.R. Non-fullerene acceptor organic photovoltaics with intrinsic operational lifetimes over 30 years. *Nat. Commun.* **2021**, *12*, 5419. [[CrossRef](#)] [[PubMed](#)]
13. Georgiou, E.; Papadas, I.T.; Antoniou, I.; Oszajca, M.F.; Hartmeier, B.; Rossier, M.; Luechinger, N.A.; Choulis, S.A. Antimony doped tin oxide/polyethylenimine electron selective contact for reliable and light soaking-free high performance inverted organic solar cells. *APL Mater.* **2019**, *7*, 91103. [[CrossRef](#)]
14. Ioakeimidis, A.; Hauser, A.; Rossier, M.; Linardi, F.; Choulis, S.A. High-performance non-fullerene acceptor inverted organic photovoltaics incorporating solution processed doped metal oxide hole selective contact. *Appl. Phys. Lett.* **2022**, *120*, 233301. [[CrossRef](#)]
15. Sorrentino, R.; Kozma, E.; Luzzati, S.; Po, R. Interlayers for non-fullerene based polymer solar cells: Distinctive features and challenges. *Energy Environ. Sci.* **2021**, *14*, 180–223. [[CrossRef](#)]
16. Shrotriya, V.; Li, G.; Yao, Y.; Chu, C.W.; Yang, Y. Transition metal oxides as the buffer layer for polymer photovoltaic cells. *Appl. Phys. Lett.* **2006**, *88*, 73508. [[CrossRef](#)]
17. Irwin, M.D.; Buchholz, D.B.; Hains, A.W.; Chang, R.P.H.; Marks, T.J. p-Type semiconducting nickel oxide as an efficiency-enhancing anode interfacial layer in polymer bulk-heterojunction solar cells. *Proc. Natl. Acad. Sci. USA* **2008**, *105*, 2783–2787. [[CrossRef](#)]
18. Han, S.; Shin, W.S.; Seo, M.; Gupta, D.; Moon, S.J.; Yoo, S. Improving performance of organic solar cells using amorphous tungsten oxides as an interfacial buffer layer on transparent anodes. *Org. Electron.* **2009**, *10*, 791–797. [[CrossRef](#)]
19. Wang, K.; Ren, H.; Yi, C.; Liu, C.; Wang, H.; Huang, L.; Zhang, H.; Karim, A.; Gong, X. Solution-processed Fe₃O₄ magnetic nanoparticle thin film aligned by an external magnetostatic field as a hole extraction layer for polymer solar cells. *ACS Appl. Mater. Interfaces* **2013**, *5*, 10325–10330. [[CrossRef](#)]
20. Yu, Z.; Liu, W.; Fu, W.; Zhang, Z.; Yang, W.; Wang, S.; Li, H.; Xu, M.; Chen, H. An aqueous solution-processed CuO_x film as an anode buffer layer for efficient and stable organic solar cells. *J. Mater. Chem. A* **2016**, *4*, 5130–5136. [[CrossRef](#)]
21. Gama, L.; Ribeiro, M.A.; Barros, B.S.; Kiminami, R.H.A.; Weber, I.T.; Costa, A.C.F.M. Synthesis and characterization of the NiAl₂O₄, CoAl₂O₄ and ZnAl₂O₄ spinels by the polymeric precursors method. *J. Alloys Compd.* **2009**, *483*, 453–455. [[CrossRef](#)]
22. Xu, H.; Xu, H.; Yuan, F.; Zhou, D.; Liao, X.; Chen, L.; Chen, Y.; Chen, Y. Hole transport layers for organic solar cells: Recent progress and prospects. *J. Mater. Chem. A* **2020**, *8*, 11478–11492. [[CrossRef](#)]
23. Wu, Z.; Zhu, Y.; Ji, X. NiCo₂O₄-based materials for electrochemical supercapacitors. *J. Mater. Chem. A* **2014**, *2*, 14759–14772. [[CrossRef](#)]
24. Papadas, I.T.; Ioakeimidis, A.; Armatas, G.S.; Choulis, S.A. Low temperature combustion synthesis of a spinel NiCo₂O₄ hole transport layer for perovskite photovoltaics. *Adv. Sci.* **2018**, *5*, 1701029. [[CrossRef](#)] [[PubMed](#)]
25. Dalas, E.; Mougoyannis, P.; Sakkopoulos, S. Effect of ZnO concentration on the structure and charge transport in conductive polypyrrole/ZnO x% w/w composites with x = 10, 20, 30 and 40. *Rom. J. Phys.* **2013**, *58*, 354–364.
26. Dileep, K.; Loukya, B.; Silwal, P.; Gupta, A.; Datta, R. Probing optical band gaps at nanoscale from tetrahedral cation vacancy defects and variation of cation ordering in NiCo₂O₄ epitaxial thin films. *J. Phys. D Appl. Phys.* **2014**, *47*, 405001. [[CrossRef](#)]
27. Hu, L.; Wu, L.; Liao, M.; Fang, X. High-performance NiCo₂O₄ nanofilm photodetectors fabricated by an interfacial self-assembly strategy. *Adv. Mater.* **2011**, *23*, 1988–1992. [[CrossRef](#)]
28. Hu, L.; Wu, L.; Liao, M.; Hu, X.; Fang, X. Electrical transport properties of large, individual NiCo₂O₄ nanoplates. *Adv. Funct. Mater.* **2012**, *22*, 998–1004. [[CrossRef](#)]

29. Vitoratos, E.; Sakkopoulos, S.; Dalas, E.; Paliatsas, N.; Karageorgopoulos, D.; Petraki, F.; Kennou, S.; Choulis, S.A. Thermal degradation mechanisms of PEDOT:PSS. *Org. Electron.* **2009**, *10*, 61–66. [[CrossRef](#)]
30. Vitoratos, E.; Sakkopoulos, S.; Dalas, E.; Emmanouil, K. Conductivity Degradation Study of polypyrrole and polypyrrole/5% w/w TiO₂ nanocomposite under Heat Treatment in Helium and Atmospheric Air. *Int. J. Eng. Appl. Sci.* **2016**, *3*, 13–16.

Disclaimer/Publisher's Note: The statements, opinions and data contained in all publications are solely those of the individual author(s) and contributor(s) and not of MDPI and/or the editor(s). MDPI and/or the editor(s) disclaim responsibility for any injury to people or property resulting from any ideas, methods, instructions or products referred to in the content.